Proceedings of ISFOG 2025
5TH INTERNATIONAL SYMPOSIUM ON
FRONTIERS IN OFFSHORE GEOTECHNICS
Nantes, France | June 9-13 2025

ISBN 978-2-85782-758-0

A novel machine learning method for processing of P and S suspension logging data

J.W. Buist*
Fugro, Nootdorp, The Netherlands

J.G. Burgers, P.J. Maas
Fugro, Nootdorp, The Netherlands

j.buist@fugro.com

ABSTRACT: P-wave and S-wave velocities are used as input for calculating key parameters for offshore foundation design, such as small strain shear modulus, and as input for enhancement of seismic reflection data. P and S suspension logging (PSSL) is a common borehole geophysical logging technique for deriving these velocities in soil and rock. The PSSL tool generates acoustic waves in the borehole and records them, as a trace pair, at two receivers with different spacings from the source. P- and S-wave velocities are derived from the difference in arrival times of the acoustic waves at both receivers. Typically, a competent human user picks the arrival times, i.e. manual picking, which is a time-consuming exercise. This paper presents a machine learning algorithm, known as P and S Interpretation Network (PSINET), that automates the picking process. The algorithm output consists of picked arrival times for both P- and S-wave data, from which the acoustic velocities are derived. PSINET is a deep neural network, trained with a dataset of more than 100,000 manually picked and reviewed PSSL trace pairs. The use of PSINET has been successfully piloted on a public domain dataset (blind data). Results of this campaign show that PSINET predicts correct outputs for 86% of the P-wave data and 44% of the S-wave data. Review by a competent user is still required. PSINET reduces deliverables turnaround time and decreases the influence of interpreter bias. Further training of PSINET is planned to cover a wider range of ground conditions.

Keywords: P and S suspension logging; neural networks; acoustic waves; borehole geophysical logging; machine learning

1 INTRODUCTION

Compressional and shear wave velocities, commonly referred to as P-wave velocity (v_p) and S-wave velocity (v_s), are used as input for calculating key parameters for offshore foundation design, such as the small strain modulus, Young's modulus and Poisson's ratio (Masters et al., 2019). Furthermore, these velocities can be applied for other applications such as enhancing offshore seismic reflection data by updating the velocity model.

One method for deriving P- and S-wave velocities is P and S suspension logging (PSSL), a common borehole geophysical logging method in accordance with ISO 19901-8:2023 (2023). Driven by the growth of the offshore wind industry, PSSL data volumes have risen rapidly over the past years. The increase of available manually processed data opened the way for training a deep neural network for PSSL data picking.

This paper presents a deep convolutional neural network algorithm, known as P and S Interpretation Network (PSINET), for automated PSSL data processing. PSINET is a patented technology. In Section 2, a concise overview of PSSL data acquisition and manual processing is provided as necessary for understanding the automated processing algorithm. Section 3 describes the architecture of PSINET as well as the training and testing thereof, using Fugro's catalogue of available P-, S1-, and S2-wave arrival times picked and reviewed by competent users. Section 4 presents the results of automated processing using PSINET compared with manually processed results on a large dataset from the public domain (Fugro, 2024a, 2024b). Section 5 discusses the performance of PSINET and other algorithms for processing of acoustic data.

2 P AND S SUSPENSION LOGGING

2.1 Data Acquisition

The PSSL tool (Figure 1) consists of an acoustic dipole source and two receivers with different spacings relative to the source. The source and receivers are acoustically isolated to prevent transmission of direct tool arrivals. The dipole source generates acoustic waves in the borehole, including a refracted P-wave and a flexural wave. The dipole source is fired in two opposite directions to generate flexural waves with opposite polarity. The acoustic waves are detected at the tool's receivers, where the "near" receiver is closer to the source than the "far" receiver. The receivers are spaced at a fixed distance from each other, usually 1.0 m.

Figure 1: Schematic drawing of the PSSL tool with annotated source, receivers, and acoustic isolator sections.

During acquisition, "acquisition cycles" are performed at each test depth ("station") in the borehole. One acquisition cycle generates three recorded trace pairs with one trace pair (or "shot") for each of the three data types (or "modes"): P-wave mode relating to the refracted P-wave, and S1-wave and S2-wave modes corresponding to the two flexural waves of opposite polarity.

The signal quality of the recorded data may be affected by factors such as ground, borehole, and environmental conditions. Thus, it is recommended practice to perform multiple acquisition cycles per station, typically five to ten, to optimize data quality (Burgers et al., 2025).

2.2 Manual Data Processing

P- and S-wave velocities can be derived from the difference in arrival times of the acoustic signals at the near and far receivers in conjunction with the known receiver spacing. A user determines the arrival times by manual picking, i.e. the manual processing of PSSL data referred to in this paper. This manual process can be time-consuming and requires training and experience for competency and consistency.

For quality checks, multiple shots (usually three) are processed for each mode per station. On a single station, this process yields multiple shot velocities for the P-wave, S1-wave, and S2-wave modes. These are averaged into a single station velocity per mode. Where applicable, the average of the S1- and S2-wave velocities is considered the S-wave velocity.

Typically, the three processed shots per mode are those assessed by the user as the best quality data with the least noise impact; the other shots on the station are left unprocessed. Each mode may be processed using different acquisition cycles. Generally, S-wave data are more difficult to process than P-wave data. Thus, S-wave data are deemed of insufficient quality for velocity derivation more often than P-wave data.

Even for competent users, it can be challenging to pick the exact same velocity on two different shots on a station. Percentage-based repeatability limits are imposed to ensure the derived velocities for each wave type (P-wave and S-wave) are repeatable, where consideration is given to higher relative variance in lower derived velocities. Thus, a staggered approach as presented in Table 1 is used, where v_{max} is the maximum picked velocity for the wave type at the station. In this paper, these velocity repeatability limits are used to assess PSINET's predictions as described in Section 3.4.

Table 1. Velocity repeatability limits (Burgers et al., 2025)

Maximum Wave Velocity [m/s]	Repeatability Limit
$v_{max} < 500$	10%
$500 \leq v_{max} < 1500$	5%
$v_{max} \geq 1500$	3%

Furthermore, each picked mode per station is assigned a confidence class according to multiple criteria assessing trace interpretability (Burgers et al., 2025). The four confidence classes include C1 (High), C2 (Medium), C3 (Low), and C4 (Insufficient). Confidence class is used in this study as a measure of the complexity of the data given to PSINET for testing.

3 P AND S INTERPRETATION NETWORK

3.1 Architecture

Recent accomplishments have been made by adapting the popular medical segmentation network U-Net (Ronneberger et al., 2015) into a neural network for phase picking and earthquake detection (PhaseNet), thereby achieving much higher picking accuracy than previously existing methods (Zhu and Beroza, 2018). Building upon these recent developments, this study adapts the U-Net architecture for PSSL picking.

PSINET is a deep convolutional neural network which is designed to produce a segmentation from PSSL recordings. The segmented output is equal to 1 for the time interval between the estimated near and far receiver arrivals, and equal to 0 before the arrival on the near receiver and after the arrival on the far receiver. The timestamp where the segmentation flips from 0 to 1 corresponds with the picked arrival on the near receiver and where the segmentation flips back from 1 to 0 corresponds with the picked arrival on the far receiver. This is illustrated in Figure 2.

Two different versions of PSINET were developed. For P-waves, the near and far recordings are used as a dual-channel input; for S-Waves, PSINET uses the near and far recordings from the S1 and S2 modes together as a quad-channel input. The output is the same single-channel segmentation in both versions, i.e. it generates one segmentation for the P-wave input

and one segmentation for the combined S1- and S2-wave input.

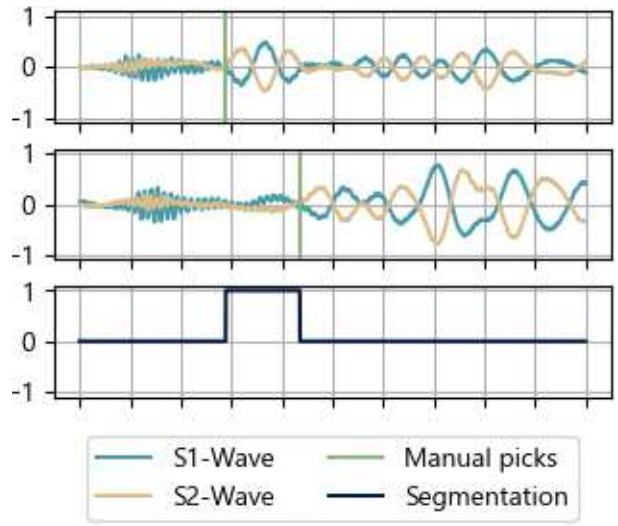

Figure 2: From top to bottom, all on the same time axis: Near receiver recording, far receiver recording, and segmentation defined from manual picks. Both recordings consist of a S1 and S2 mode.

3.2 Training Data

Training of the network proved the most successful while using the Generalized Intersection over Union (GIoU) loss function. The GIoU is a generalized version of the Intersection over Union (IoU) loss, also known as the Jaccard index, which is defined as the intersection size divided by the union size and quantifies similarity (Rezatofighi et al., 2019). This loss function has the benefit that it is stricter on the size (length) of the segmentation than on its actual location compared to other common loss functions such as the mean absolute error (MSE). For the PSSL data segmentation presented here (Figure 2), the size of the segmented part corresponds directly with the desired result: the arrival time difference between the receivers used to derive the acoustic velocity.

A substantial dataset was compiled for the training of PSINET, including data from over 20 different projects which were mainly conducted in the North Sea. Most data come from projects where the ground conditions consist of sands, transitional soils and clays. In terms of derived velocity data, 50% of available P-wave data are between 1674 m/s and 1818 m/s and 50% of available S-wave data are between 260 m/s and 399 m/s. In total, the dataset included roughly 45,000 P-wave, 40,000 S1-wave, and 40,000 S2-wave picked shots, all processed by competent users.

A Kernel Density Estimation (KDE), which is a smooth, continuous estimate of the probability density function of a random variable, is presented for the training data and the testing data (Section 3.3) for P-waves in Figure 3 and for S-waves in Figure 4. The KDE is computed by summing up kernel functions centred at each data point using Scott‘s Rule for Gaussian kernel size estimation (Scott, 2015). The main portion of the distribution is presented, excluding outliers, to emphasize the primary characteristics of the data. Both figures are presented on the same density scale to ensure comparability.

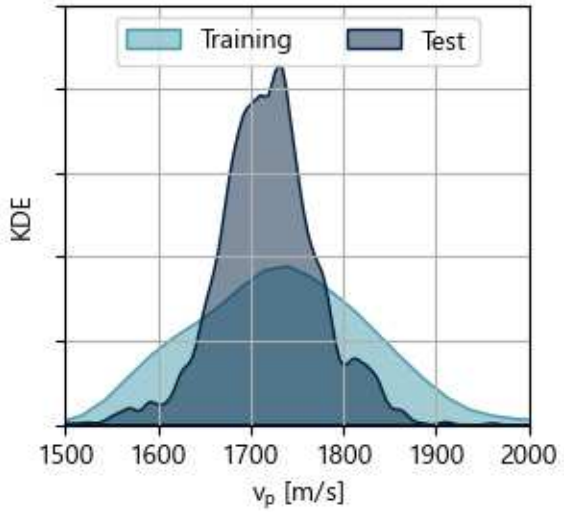

Figure 3: KDE’s for P-wave data in the training and the testing datasets.

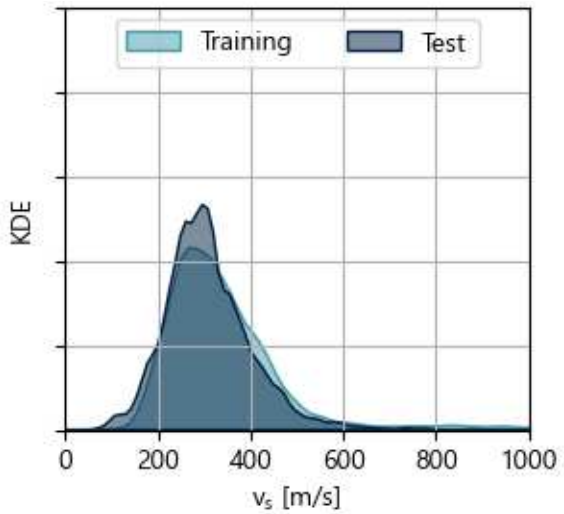

Figure 4: KDE’s for S-wave data in the training and the testing datasets.

During the training of PSINET, the training dataset was randomly split into 80% for training and 20% for validation. Actual performance was tested on data from an unseen project with a variety of soils.

On-the-fly data augmentations were applied during training to further improve the network’s robustness. Augmentation types were chosen based on their ability to mimic real features in the data. The following types of augmentation were utilised:

- Mirroring the acoustic data over the time axis (reversing signal polarity)
- Baseline shifts mimicking constant noise
- Random muting of parts of the input signal
- Addition of Gaussian noise – to replicate electronic noise, for example
- Time shifts - these make the network more robust to earlier and later arrivals.

3.3 Testing Data

A testing dataset was compiled with PSSL data from two geotechnical campaigns carried out by Fugro for the Netherlands Enterprise Agency (RVO) in 2023: IJmuiden Ver Wind Farm Sites V-VI (IJVWFS V-VI) and Nederwiek Wind Farm Site I (NWWFS I). There are no data present in the training dataset from these locations. All stations where P- or S-wave velocities were presented in the report were used in the testing dataset. All shot records at these stations, picked or unpicked, were included.

Figure 3 and Figure 4 present KDE's of the picked shots in the testing dataset. While not clearly visible for S-waves, Figure 3 shows a narrower spread in P-wave velocities in the testing dataset compared with the training dataset, due to the testing dataset having less soil variability.

In total, the testing dataset consists of 5487 P-wave and 3894 S-wave picked shots, with on average per station: 11 shots present, three P-wave shots picked, and four S-wave shots picked. In the ideal case, where all modes are picked three times for each station, there should be six S-wave picked shots per station. The higher difficulty of processing S-wave data is confirmed by the lower number of picked S-wave stations than expected and the confidence levels assigned to the picked stations. For P-wave, the average confidence class is C1 (high) on both sites; for S-wave, the confidence class averages C3 (low) for IJVWFS V-VI and C2 (medium) for NWWFS I.

3.4 Performance Metrics

For each of the manually picked shots, it is possible to perform a direct comparison with PSINET's output by computing a relative error defined as:

$$E = \frac{|v_{manual} - v_{pred}|}{v_{manual}} * 100 \qquad (1)$$

where E is the relative error between the manually picked velocity v_{manual} and the PSINET-predicted velocity v_{pred}. While the relative error tells us something about the network's performance, it is not a good indicator of practical usability.

By combining the staggered velocity repeatability scheme introduced in Section 2.2 with the relative error, a more practical metric can be introduced, namely the Pick Success Ratio (PSR). PSR is defined as the ratio of the total manual picks in the dataset where PSINET produces a correct velocity prediction. Here, the correct velocity is defined as a velocity inside the velocity repeatability margin of the manually picked shot velocity. The applicable velocity repeatability limit is determined as per Table 1, where now v_{manual} is considered instead of v_{max}.

PSINET provides a pick for every shot in the test data, i.e. also for the shots that have not been manually picked. Therefore, an alternative comparison approach can be used that also includes those unpicked shots in the testing dataset. For each of the shots in a station, manually picked or unpicked, PSINET's output is compared with the average velocity of the manually picked shots. If no picks were made for a particular mode on a station, it is not considered. A station is assessed as correct, when PSINET can produce at least three picks within the velocity repeatability limit of the average manual velocity. The total ratio of correctly processed stations by PSINET divided by the total amount of manually picked stations is defined as the Station Success Ratio (SSR).

Finally, it is also possible to apply PSINET on each shot and compare the predicted velocity directly with the manually picked average velocity for each station. This metric, the Total Success Ratio (TSR), is defined as the ratio between the amount of PSINET picks within the velocity repeatability limit divided by the total amount of shots in the dataset. However, this metric is regarded as overly pessimistic as shots that would be considered unsuitable for velocity derivation by a human user, e.g. data with obstructive levels of noise, are included in the analysis. Therefore, the TSR was not used to assess PSINET's performance.

4 RESULTS

Table 2 presents the average relative error (E_{avg}), the PSR, and the SSR for the P-wave version of PSINET. These metrics are presented for the S-wave version in Table 3. For P-waves, the network performs well with an overall SSR of 85.7%. The S-wave model correctly processes the data with an overall SSR of 44.2%. The lower performance of the S-wave model was anticipated, given the higher complexity of the S-wave data compared to the P-wave data. The SSR is mostly higher than the PSR, except for the S-wave data of IJVWFS V-VI. In this case, additional manual picks were placed on some stations with low complexity data, thus positively skewing the PSR result.

Table 2. PSINET performance metrics for P-waves

Site	E_{avg}	PSR	SSR
IJVWFS V-VI	2.1%	82.5%	87.9%
NWWFS I	2.7%	76.0%	83.7%
Overall	**2.4%**	**79.2%**	**85.7%**

Table 3. PSINET performance metrics for S-waves

Site	E_{avg}	PSR	SSR
IJVWFS V-VI	20.5%	38.0%	33.6%
NWWFS I	21.1%	34.1%	59.2%
Overall	**20.8%**	**36.0%**	**44.2%**

Figure 5 and Figure 6 below show examples of P-wave and S-wave data correctly labelled by PSINET, respectively. In the S-wave example, there is a time shift in the picking approach of PSINET versus the manually placed picks. It is important to note here that, while the picked arrival times on Figure 6 may differ, the automatic derived velocity is still within limits; PSINET is merely using a different picking strategy compared to the manual picking.

5 DISCUSSION

In the seismic industry, various algorithms have been developed to help with the manual picking of seismic arrivals, events, or phases. Traditional algorithms to automatically pick seismic arrivals include the short-term average long-term average algorithm (STA/LTA), phase arrival identification-kurtosis (PAI-K), and cross correlation pickers (Zhou et al., 2019). While most of these methods could be applied to PSSL data, few have been successfully implemented. Many of the traditional algorithms, such as the STA/LTA method, are not practically robust and introduce large biases from the desired picks (Lin and Lin, 2016). Although Lin and Lin achieved good results with a semi-empirical implementation of PAI-K, their method was not implemented in this study. The expected outcome of this study was that using a machine learning (ML) algorithm would improve output accuracy and would provide the most robust solution to various ground types.

The first ML algorithms that were widely used in the seismic industry are the traditional artificial neural networks (ANN), however with the arrival of increased computing power and deep convolutional neural networks (CNN), they were outperformed (Zhou et al., 2019). Besides CNN architectures, Recurrent Neural Networks (RNN) and Long Short-Term Memory (LSTM) networks are also prospective methods for PSSL processing, partially because of their suitability to sequential data. In this study, one specific CNN architecture (U-Net) was adapted for PSSL processing and no other architectures were further investigated.

Various techniques specific for downhole acoustic arrival picking exist, such as threshold-based detection and semblance processing (e.g. Lang et al., 1987). These algorithms, widely used for the processing of data from monopole and dipole sonic wireline tools, are not promising for PSSL data. PSSL data can be noisy, making threshold-based detection unreliable. Semblance algorithms are not suitable, since the desired acoustic arrival in PSSL data is typically accompanied by other undesired arrivals.

6 CONCLUSION

Results of the first test of PSINET on a large dataset show that PSINET predicts correct outputs for 86% of the P-wave data and 44% of the S-wave data. The results are promising and significant time savings in processing can be achieved. By requiring less manual input, PSINET also paves the way to reducing interpreter bias.

In the current workflow, PSINET can be used as the initial processing step for PSSL data, where it is used to automatically processes an unprocessed dataset after data acquisition. Thus, the initial manual processing by a competent user is not required. It takes the algorithm less than one minute to process 100 stations of P-, S1-, and S2-wave data on a standard business laptop.

After applying the model, a competent user reviews the automatic picks and adjusts them where required. Based on the performance of the currently available versions, the use of PSINET to perform the initial automated picking reduces total processing time by approximately 20-40%, as compared to the completely manual approach, depending on the difficulty of the dataset.

For future work, the performance of PSINET can be improved by adding more data to the training dataset. Moreover, it would be beneficial to include a larger variety of soils in the training data; the current training dataset is only sparsely populated with higher velocity soils. Furthermore, pairing the training and testing datasets with additional soil information from integrated datasets would benefit further analysis and dataset normalization over soil types. Well paired data is not always available, with the exception of natural gamma data.

In addition to further development of the soil models, research is planned to train a separate model with data acquired in rock formations as it may be difficult to create a well-balanced dataset of both soil and rock data due to the differing volumes available.

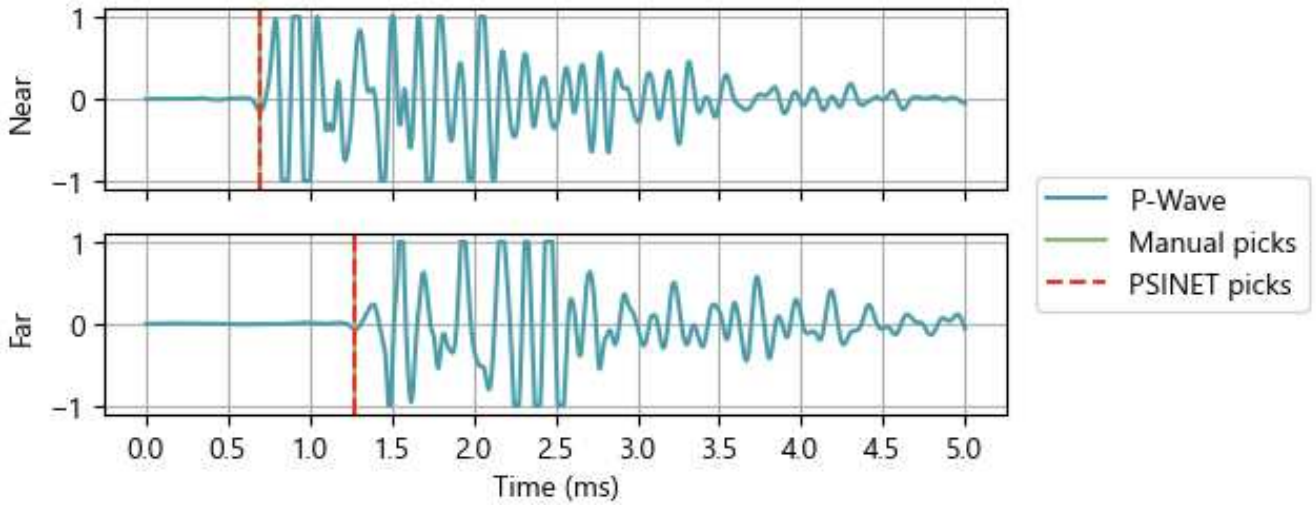

Figure 5 - Example of P-wave recording with manual and PSINET picking ($v_{manual} = 1736\ m/s$, $E = 0.7$).

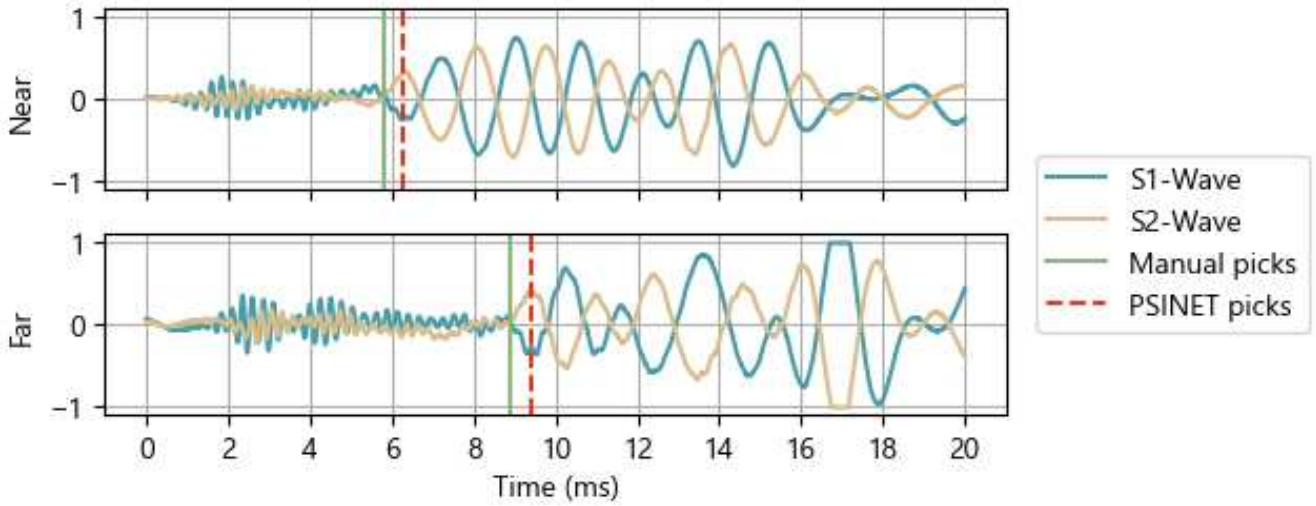

Figure 6 - Example of S-wave recording with manual and PSINET picking ($v_{manual} = 323\ m/s$, $E = 1.7$).

AUTHOR CONTRIBUTION STATEMENT

J.W. Buist: Conceptualization, Data curation, Formal analysis, Methodology, Software, Writing - original draft. **J.G. Burgers**: Conceptualization, Project Administration, Writing – reviewing and editing. **P.J. Maas**: Supervision, Writing - reviewing and editing.

ACKNOWLEDGEMENTS

The authors acknowledge the Netherlands Enterprise Agency (RVO) for their kind permission to use data acquired by Fugro during the geotechnical site investigations performed for RVO on IJVWFS V-VI and NWWFS I.

REFERENCES

Burgers, J., Maas, P., Buist, J., & Peuchen, J. (2025). A confidence classification scheme for P and S suspension logging data. To be published at: *5th International Symposium on Frontiers in Offshore Geotechnics*, Nantes, France.

Fugro (2024a). Investigation Area IJmuiden Ver Wind Farm Sites V & VI – Investigation results geotechnical borehole locations, Fugro Netherlands Marine B.V., Nootdorp, The Netherlands, Fugro Report: IJ56_20240705_GT_FNLM_Geotechnical Borehole Locations_V03_D, issued 5 July 2024 to RVO.

Fugro (2024b). Investigation Area Nederwiek Zuid – Investigation results geotechnical borehole locations. Fugro Netherlands Marine B.V., Nootdorp, The Netherlands, Fugro Report: NWZ_20240916_GT_FNLM_Geotechnical Borehole Locations_V02_P, issued 16 September 2024 to RVO.

International Organization for Standardization (2023). ISO 19901-8:2023 Oil and gas industries including lower carbon energy – offshore structures – part 8: marine soil investigations, ISO, Switzerland.

Lang, S. W., Kurkjian, A. L., McClellan, J. H., Morris, C. F., & Parks, T. W. (1987). *Estimating slowness dispersion from arrays of sonic logging waveforms*. Geophysics, 52(4), pp. 530-544. https://doi.org/10.1190/1.1442322

Lin, C. H., & Lin, C. P. (2016). Phase velocity approach for Suspension P–S Logging data analysis. *Journal of Applied Geophysics*, *129*, pp. 126-132. https://doi.org/10.1016/j.jappgeo.2016.04.001

Masters, T. A., Juszkiewicz, P., Mandolini, A., Christian, H. (2019). A Critical Appraisal of the Benefits of and Obstacles to Gaining Quality Data with Offshore Seismic CPT and P-S Logging, In: *Offshore Technology Conference*, Houston, USA, pp. 364-377. https://doi.org/10.4043/29485-MS

Rezatofighi, H., Tsoi, N., Gwak, J., Sadeghian, A., Reid, I., & Savarese, S. (2019). Generalized intersection over union: A metric and a loss for bounding box regression. In: *Proceedings of the IEEE/CVF conference on computer vision and pattern recognition*, pp. 658-666. https://doi.org/10.48550/arXiv.1902.09630

Ronneberger, O., Fischer, P., & Brox, T. (2015). U-net: Convolutional networks for biomedical image segmentation. In: *Medical image computing and computer-assisted intervention–MICCAI 2015: 18th international conference, Munich, Germany,* pp. 234-241. https://doi.org/10.1007/978-3-319-24574-4_28

Scott, D. W. (2015) *Multivariate Density Estimation: Theory, Practice, and Visualization*, 2nd ed., John Wiley & Sons, Hoboken, United States of America. https://doi.org/10.1002/9781118575574

Zhou, Y., Yue, H., Kong, Q., & Zhou, S. (2019). Hybrid event detection and phase-picking algorithm using convolutional and recurrent neural networks. *Seismological Research Letters*, 90(3), pp. 1079-1087. https://doi.org/10.1785/0220180319

Zhu, W., & Beroza, G. C. (2019). PhaseNet: a deep-neural-network-based seismic arrival-time picking method. *Geophysical Journal International*, 216(1), pp. 261-273. https://doi.org/10.1093/gji/ggy423